NUMERICAL SIMULATION OF THE ENDWALL HEAT TRANSFER
IN THE LANGSTON CASCADE

Alexander M. Levchenya[1], Evgueni M. Smirnov[1], and Dmitry K. Zaytsev[1,*]

[1] Department of Aerodynamics
St. Petersburg State Polytechnic University, Russia
([*] Corresponding author: aero@phmf.spbstu.ru)

CFD analysis is a powerful tool to obtain detailed data on the flow structure and heat transfer in turbine cascades. However, a systematic work has to be performed in order to validate CFD models including selection of a turbulence model, specifying adequate inlet conditions, evaluation of the grid dependence, etc. At that, among other data of practical interest, the local heat transfer is most sensitive to peculiarities of secondary flows and, consequently, to details of physical and computational modelling.

Experimental data obtained by Langston et al. [1977], Graziani et al. [1980], and Holley et al. [2006] for flows in a large-scale turbine blade cascade are selected for validation of CFD results in the present contribution. Similar CFD efforts were made previously by many authors (e.g., Ameri et al. [1994], Lee et al. [1997], Ivanov et al. [2002], Levchenya et al. [2006, 2007]) using different computational grids, numerical schemes, and turbulence models. Generally, the experience accumulated evidences that, a practically grid-independent pressure and velocity distribution can be obtained with computational grids of about half million cells and a solver of second order spatial discretization. However, in order to get grid-independent data on the local heat transfer one needs much finer grids. Moreover, the solution obtained can be affected by the turbulence model, mainly because the multi-vortex 3D flow structure at the junction between the endwall and the blade leading edge is especially sensitive to the level of the eddy viscosity generated by the model.

In the present contribution, numerical simulation of 3D turbulent flow and heat transfer in the Langston cascade has been performed using fine computational grids with applying two low-Re turbulence models, those by Wilcox [1993] and Menter [1994]. The results obtained with the two models are compared with each other and with the above mentioned experimental data.

The cascade geometry shown in Fig. 1 is defined in accordance with the experiment conditions. In particular, the cascade axial width is $b_x = 281.3$ mm, the blade chord is equal to $1.2242\,b_x$, pitch $0.9555\,b_x$, span $0.9888\,b_x$. The inlet flow angle is 44.7°, the core velocity $V_{in} = 33.5$ m/s. The flow is treated steady state and incompressible, the air physical properties are defined at the inlet temperature ($T_{in} = 293$ K) and atmospheric pressure; the Reynolds number $Re = b_x V_{in}/\nu = 6.45 \times 10^5$, the Prandtl number $Pr = 0.72$.

The flow periodicity along the blade pitch is assumed and the mirror symmetry boundary condition is used at the mid-span plane. A uniform static pressure is applied at the domain exit section. The inlet distributions of the flow velocity and turbulence characteristics are specified on the base of auxiliary computations of 2D boundary layer in a parallel-plate channel so that to fit the experimental data on the endwall boundary layer thickness at the working section inlet. The input heat flux at the blade surface and at the heated part of the endwall ($0.22b_x$ upstream and downstream of the blade edges) is

defined as 0.131W/cm^2 and 0.183W/cm^2 respectively; the other part of the endwall is treated adiabatic.
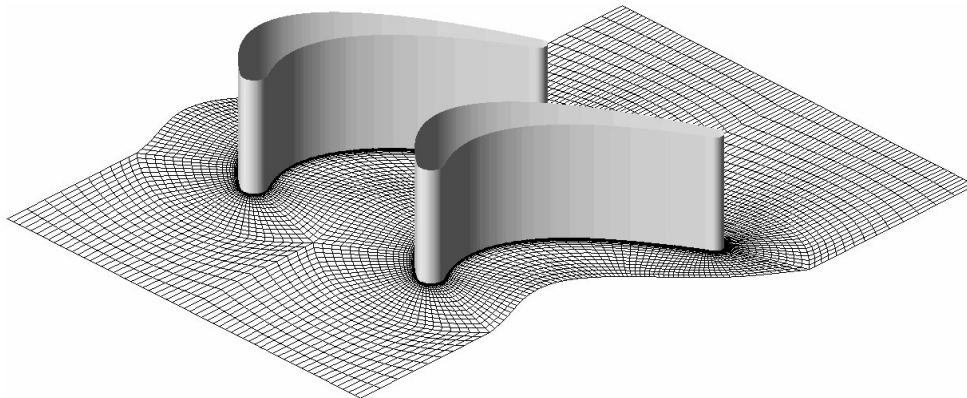

Figure 1. Blade channel configuration and the endwall computational grid

The computational grid is illustrated in Fig. 1 (every second grid line at the endwall is shown). The grid contains 1.1 million cells; the number of grid nodes along the blade profile is about 400. The near-wall grid spacing is $10^{-4}\,b_x$ that provides the value of y^+ about and below unity throughout the walls. The computations have been performed with 3D Navier-Stokes solver SINF [e.g. Smirnov, 2004] using the second order spatial discretization by means of the finite volume method. The simulation results obtained are nearly grid independent.

The measured and computed limiting streamlines on the endwall are shown in Fig. 2. As compared to the k-ω model, the SST model yields a more complex flow structure with an additional counter rotating secondary vortex positioned slightly upstream (and closer to the wall) of the horseshoe vortex. This secondary vortex results in a specific strip in the streamline pattern (downstream of the main flow separation line passing through the saddle point) that is not observed in the experiment, probably because of insufficient spatial resolution of the measurements or/and a weak unsteadiness of this zone. However apart from this local distinction, the SST model provides better agreement with the measurement results. In particular, the k-ω model predicts inadequate inclination of the limiting streamlines in the middle of the channel.
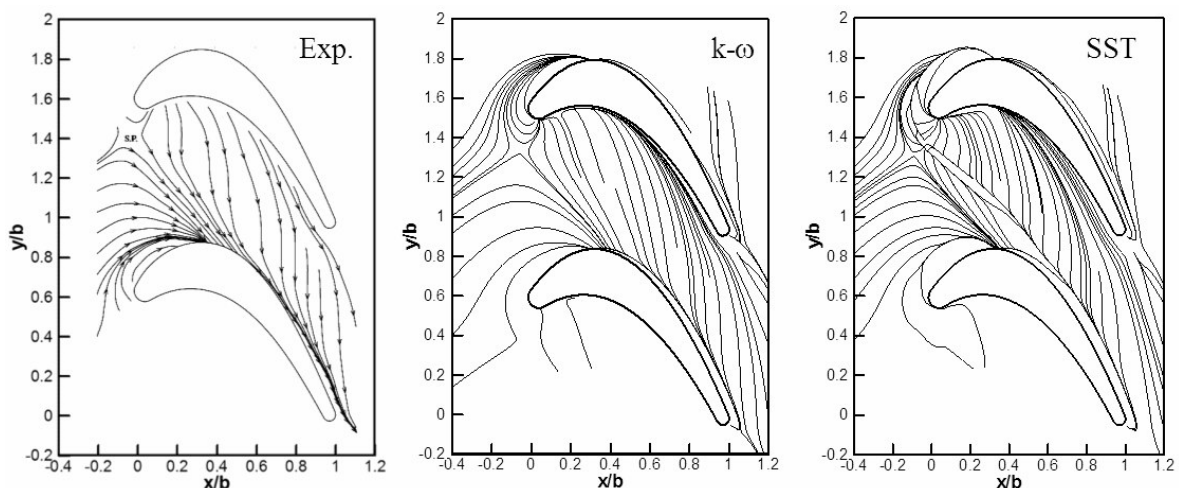

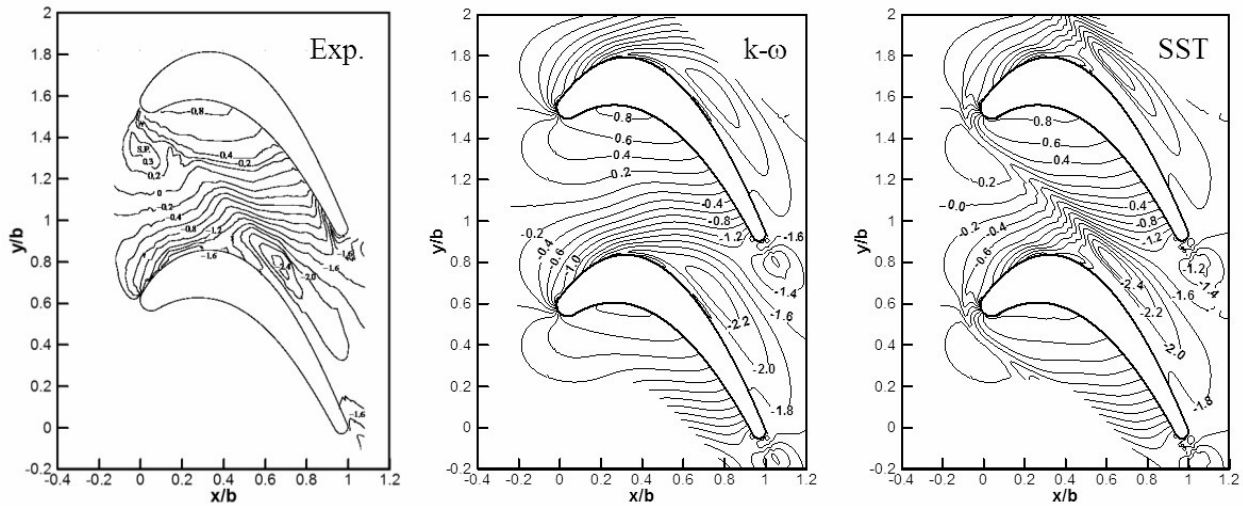Figure 2. Limiting streamlines on the endwall

Figure 3. Endwall distribution of the static pressure coefficient

Distribution of the static pressure over the endwall presented in Fig. 3 evidences that the secondary vortex predicted by the SST model does really exist. An imprint of this vortex is clearly seen in the measured pressure map as a comb-shaped concentration of the isolines due to local depression in the vortex. Quite similar (slightly more pronounced) depression along the secondary vortex is present in the solution obtained with the SST model. Unlike that, in the k-ω model solution, the secondary vortex is not reproduced (because of a much higher level of the eddy viscosity in the boundary layer) and, consequently, there is no associated strip of depression in the plot.
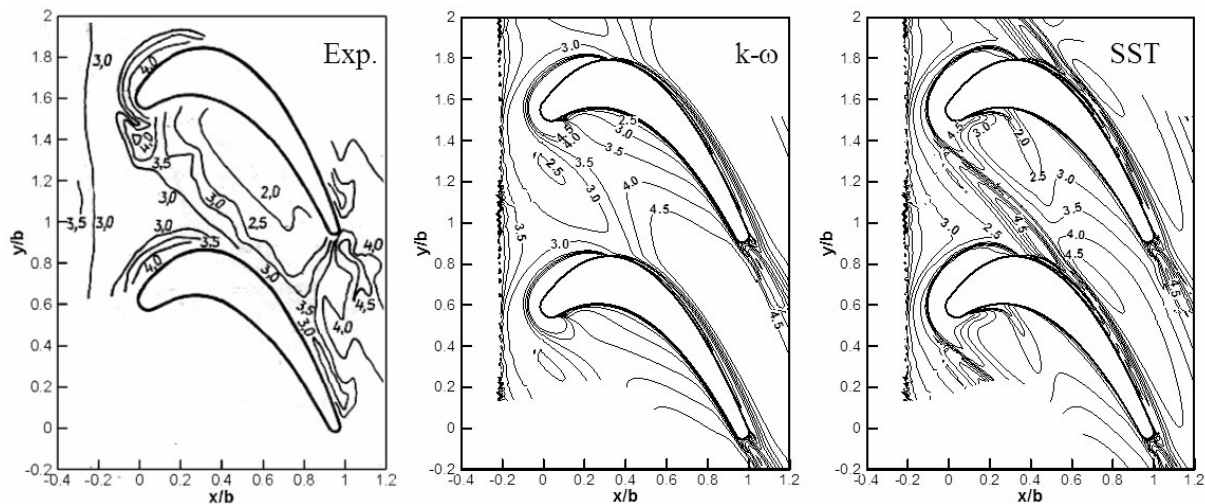

Figure 4. Distribution of Stanton number ($St \times 10^3$) over the endwall

Figure 4 presents the endwall heat transfer data obtained. Taking into account the complexity of the phenomenon modeled, the agreement between the measurement and the computation results can be regarded as satisfactory. Again, the SST model provides better prediction of some characteristic features of the Stanton number distribution such as concentration of the isolines in the middle of the blade channel and the presence of a large zone of reduced heat transfer near the blade pressure side. However in the last third of the blade channel and farther downstream, the measured and computed

distributions of the Stanton number are essentially different. Very likely, this disagreement is due to large-scale unsteady vortices shed from rather thick trailing edge of the blade (but, naturally, not reproduced in the steady-state solution) that provide additional mixing in the blade wake and smooth the local heat transfer.

Among two flow regimes studied in the above mentioned experiments with the Langston cascade, the results presented in this abstract correspond to the case with relatively thick endwall boundary layer (of the order of the blade leading edge thickness). Similar computations (to be presented in the full paper) have been performed also for the other test case with a much thinner boundary layer. For this case, the 3D effects are less pronounced (in particular, there is no secondary vortex) and both turbulence models provide better agreement with the measurements, though the SST model still keeps some superiority.

REFERENCES

Ameri, A. A., Arnone, A. [1994]. Prediction of turbine blade passage heat transfer using a zero and two-equation turbulence models. *ASME paper*. No. 94-GT-122, 8 p.

Graziani, R. A., Blair, M. F., Taylor, J. R., and Mayle, R. E. [1980]. An experimental study of endwall and airfoil surface heat transfer in a large scale turbine blade cascade. *ASME J. Eng. Power*, Vol. 102, pp. 257-267.

Holley, B. M., Langston, L. S. [2006]. Surface shear stress and pressure measurements in a turbine cascade. *Proc. ASME Turbo Expo 2006*, GT2006-90580, 10 p.

Ivanov, N. G., Levchenya, A. M., Ris, V. V., and Smirnov, E. M. [2002]. Calculation of three-dimensional flow and heat transfer in an experimental model of a blade cascade on the base of one- and two equation turbulence models. *Proc. 3rd Russian National Heat Transfer Conf.*, MPEI Publishers, Moscow, Russia, Vol.2, pp. 147-150 (in Russian).

Langston, L. S., Nice, M. L., Hooper, R. M. [1977]. Three-dimensional flow within a turbine cascade passage. *ASME J. Eng. Power*, Vol. 99, pp. 21-28.

Lee, H. G., Yoo, J. Y. [1997]. Numerical simulation of turbulent cascade flows involving high turning angles. *Computational Mechanics*, No.20, pp. 247-260.

Levchenya, A. M., Ris, V. V., and Smirnov, E. M. [2006]. Testing of turbulence models as applied to calculations of 3D flow and endwall heat transfer in cascades of thick vane blades. *Proc. 4th Russian National Heat Transfer Conf.*, MPEI Publishers, Moscow, Russia, Vol.2, pp. 167-170 (in Russian).

Levchenya, A. M., Smirnov, E. M. [2007]. CFD-analysis of 3D flow structure and endwall heat transfer in a transonic turbine blade cascade: effects of grid refinement. *CD-ROM Proc. West-East High Speed Flow Field Conference - WEHSFF'07*, Moscow, 12 p.

Menter, F. R. [1994]. Two equation eddy-viscosity turbulence models for engineering applications. *AIAA Journal*. Vol. 32. pp. 1598-1605.

Smirnov, E. M., and Zaitsev D. K. [2004]. The finite-volume method in application to complex-geometry fluid dynamics and heat transfer problems. *Scientific and Technical Bulletin of the St.-Petersburg State Technical University*, No. 2(36), pp.70-81 (in Russian).

Wilcox, D.C. [1993]. A two-equation turbulence model for wall-bounded and free-shear flows. *AIAA Paper*, AIAA-93-2905.